Article

Cell Reports

The Nuclear Receptor LXR Limits Bacterial Infection of Host Macrophages through a Mechanism that Impacts Cellular NAD Metabolism

Graphical Abstract

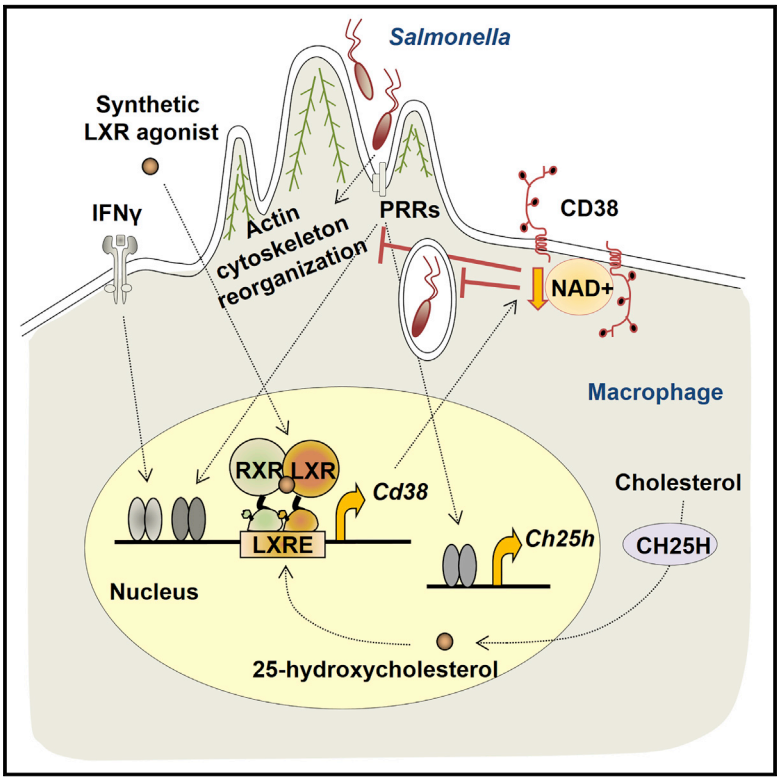

Authors

Jonathan Matalonga, Estibaliz Glaria, Mariana Bresque, ..., Antonio Castrillo, Eduardo N. Chini, Annabel F. Valledor

Correspondence

afernandezvalledor@ub.edu

In Brief

Macrophages constitute a preferential niche for intracellular bacteria to replicate. Matalonga et al. identified an antibacterial circuit mediated by pharmacological targeting of the liver X receptor (LXR) pathway that impacts intracellular NAD metabolism and interferes with macrophage cytoskeletal rearrangements subverted by invasive bacteria.

Highlights

- LXR agonists reduce intracellular NAD levels through induction of CD38
- Activation of LXRs impairs cytoskeletal changes associated with bacterial infection
- The LXR-CD38 circuit protects host macrophages from extensive bacterial infection
- Activation of the LXR-CD38 circuit ameliorates clinical signs of infection in vivo

Matalonga et al., 2017, Cell Reports *18*, 1241–1255
January 31, 2017
http://dx.doi.org/10.1016/j.celrep.2017.01.007

CellPress

Cell Reports
Article

The Nuclear Receptor LXR Limits Bacterial Infection of Host Macrophages through a Mechanism that Impacts Cellular NAD Metabolism

Jonathan Matalonga,[1] Estibaliz Glaria,[1] Mariana Bresque,[2] Carlos Escande,[2] José María Carbó,[1] Kerstin Kiefer,[3] Ruben Vicente,[3] Theresa E. León,[1] Susana Beceiro,[4] Mónica Pascual-García,[1] Joan Serret,[5] Lucía Sanjurjo,[6] Samantha Morón-Ros,[1] Antoni Riera,[7,8] Sonia Paytubi,[9] Antonio Juarez,[9,10] Fernando Sotillo,[7] Lennart Lindbom,[11] Carme Caelles,[12] Maria-Rosa Sarrias,[6] Jaime Sancho,[13] Antonio Castrillo,[4] Eduardo N. Chini,[14] and Annabel F. Valledor[1,15,*]

[1]Nuclear Receptor Group, Department of Cell Biology, Physiology and Immunology, School of Biology, University of Barcelona, Barcelona 08028, Spain
[2]Metabolic Diseases and Aging Laboratory, Institut Pasteur Montevideo, Montevideo 11400, Uruguay
[3]Laboratory of Molecular Physiology and Channelopathies, Department of Experimental and Health Sciences, Universitat Pompeu Fabra, Barcelona 08003, Spain
[4]Instituto de Investigaciones Biomédicas "Alberto Sols" de Madrid and Unidad Asociada de Biomedicina CSIC-Universidad de las Palmas de Gran Canaria (CSIC-ULPGC), Madrid 28029, Spain
[5]Experimental Toxicology and Ecotoxicology Unit, Parc Científic de Barcelona, Barcelona 08028, Spain
[6]Innate Immunity Group, Health Sciences Research Institute Germans Trias i Pujol, Badalona 08916, Spain
[7]Institute for Research in Biomedicine (IRB Barcelona), Barcelona 08028, Spain
[8]Department of Organic Chemistry, School of Chemistry, University of Barcelona, Barcelona 08028, Spain
[9]Department of Microbiology, School of Biology, University of Barcelona, Barcelona 08028, Spain
[10]Institute for Bioengineering of Catalonia (IBEC), Barcelona 08028, Spain
[11]Department of Physiology and Pharmacology, Karolinska Institutet, Stockholm SE-171 77, Sweden
[12]Department of Biochemistry and Molecular Biology, School of Pharmacy, University of Barcelona, Barcelona 08028, Spain
[13]Institute of Parasitology and Biomedicine "López-Neyra" (IPBLN), CSIC, Granada 18016, Spain
[14]Laboratory of Signal Transduction, Department of Anesthesiology and Robert and Arlene Kogod Center on Aging, Mayo Clinic College of Medicine, Rochester, MN 55905, USA
[15]Lead Contact
*Correspondence: afernandezvalledor@ub.edu
http://dx.doi.org/10.1016/j.celrep.2017.01.007

SUMMARY

Macrophages exert potent effector functions against invading microorganisms but constitute, paradoxically, a preferential niche for many bacterial strains to replicate. Using a model of infection by *Salmonella* Typhimurium, we have identified a molecular mechanism regulated by the nuclear receptor LXR that limits infection of host macrophages through transcriptional activation of the multifunctional enzyme CD38. LXR agonists reduced the intracellular levels of NAD^+ in a CD38-dependent manner, counteracting pathogen-induced changes in macrophage morphology and the distribution of the F-actin cytoskeleton and reducing the capability of non-opsonized *Salmonella* to infect macrophages. Remarkably, pharmacological treatment with an LXR agonist ameliorated clinical signs associated with *Salmonella* infection in vivo, and these effects were dependent on CD38 expression in bone-marrow-derived cells. Altogether, this work reveals an unappreciated role for CD38 in bacterial-host cell interaction that can be pharmacologically exploited by activation of the LXR pathway.

INTRODUCTION

Macrophages are essential mediators of the innate immune response. Through phagocytosis, macrophages internalize microbial pathogens, which are subsequently killed and digested in intracellular phagolysosomes (Haas, 2007). Several pathogenic microorganisms have, however, developed strategies to actively invade host cells and evade microbial digestion within the host endosomal system. In fact, despite their repertoire of microbicidal tools, macrophages represent niches in which many pathogens have established themselves for intracellular replication and dissemination (Price and Vance, 2014). For example, *Salmonella enterica* serovar Typhimurium (*S.* Typhimurium) fosters its own uptake by non-phagocytic epithelial cells and phagocytic cells, and infection and intracellular survival in macrophages is required for full virulence and dissemination (Haraga et al., 2008). Invasive *Salmonellae* strains can enter macrophages by several endocytic processes, including macropinocytosis induced by factors secreted by the type III secretion system (T3SS). Within infected host cells, the bacterium first

uses a second T3SS to transform the phagosome into a *Salmonella*-containing vacuole that supports bacterial replication and then induces macrophage pyroptosis for dissemination (Guiney and Lesnick, 2005).

Nuclear receptors are a family of ligand-activated transcription factors with diverse functions in physiology. Liver X receptors (LXRs) are nuclear receptors that can be pharmacologically activated by high-affinity agonists to subsequently regulate the expression of genes involved in lipid homeostasis. Two LXR isoforms have been identified, namely LXRα and LXRβ, both of which heterodimerize with retinoid X receptors (RXRs) to positively modulate target gene expression (Hong and Tontonoz, 2014). Apart from their metabolic functions, LXRs play important roles in the regulation of immune responses. Through different mechanisms, LXRs repress a subset of pro-inflammatory genes induced by pattern recognition receptor engagement (Ghisletti et al., 2007; Ito et al., 2015) or by interferon gamma (IFN-γ) (Pascual-García et al., 2013; Lee et al., 2009). On the other hand, the LXR pathway is involved in the acquisition of a macrophage deactivated phenotype (A-Gonzalez et al., 2009).

Based on the anti-inflammatory actions of LXR agonists, initial predictions anticipated that LXR activation could negatively impact the capability of immune cells to establish an aggressive response against pathogens. However, increased susceptibility to infection by *Mycobacterium tuberculosis* or *Listeria monocytogenes* has been observed in LXR-deficient mice (Joseph et al., 2004; Korf et al., 2009), and LXR activation prevented macrophage apoptosis induced by virulent bacteria, including *Bacillus anthracis* and *S.* Typhimurium (Valledor et al., 2004), which suggests that the LXR pathway exerts complex regulatory actions that affect microbe-host cell interaction. In this work, we have further investigated the involvement of LXR activity in immune cell function during infection by *S.* Typhimurium. Interestingly, the results reported here identify a molecular mechanism regulated by LXRs that serves to limit infection of host macrophages through modulation of cellular NAD metabolism.

RESULTS

LXR Activity Limits Macrophage Infection by *S.* Typhimurium

To investigate the role of the LXR pathway in host-pathogen interaction, we treated primary bone-marrow-derived macrophages with synthetic high-affinity LXR agonists (either TO901317 (T1317) or GW3965) and then infected the cells with *S.* Typhimurium strain SV5015 harboring the plasmid pBR.RFP.1, which encodes red fluorescent protein. Confocal fluorescence microscopy studies indicated that LXR agonists reduce the amount of intracellular bacteria and the percentage of infected macrophages after 30 min of infection (Figures 1A, S1, and S2A). Reduced bacteria burden was corroborated with flow cytometry studies (Figures 1B and S2B) and by determination of viable bacterial colony-forming units (CFUs) after macrophage cell lysis (Figure 1C). The agonists did not inhibit infection of cells deficient in LXRα and LXRβ ($LXR^{-/-}$) (Figures 1A, 1B, and S2B), indicating that the effects of these compounds were LXR dependent and LXR specific. Interestingly, the rate of intracellular bacterial replication during the first 5 hr post-infection was not altered upon LXR activation, as the differences between agonist- and vehicle-treated cells over a time-course of 5 hr were equivalent to the differences observed at 30 min of infection (Figure 1D). These results suggested that LXR activation interferes with early events during bacterial cell interaction with host macrophages. On the other hand, a time-course assay revealed that prolonged treatment with the LXR agonist is required for effective inhibition of macrophage infection (Figure 1E).

Pharmacological treatment with T1317 in vivo also reduced intracellular macrophage infection by *S.* Typhimurium in an intraperitoneal model of infection (Figure 1F). Importantly, the effects of T1317 were not indirectly mediated by any substantial decrease in the ratio of resident macrophages versus neutrophils before the infection (Figure S2C). Interestingly, the LXR agonist did not influence phagocytosis of immunoglobulin G (IgG)-opsonized *Salmonella* cells (Figure 1G), suggesting that LXR activation induces a mechanism that protects macrophages from infection by this microorganism in the absence of opsonizing antibodies.

We next determined whether LXR activation affects the internalization of other bacterial pathogens. These studies revealed that LXR activity inhibits macrophage infection by an enteroinvasive strain of *Escherichia coli* (EIEC 0124:H30) without affecting phagocytosis of non-invasive *E. coli* (Figure S2D) or internalization of Fluoresbright yellow green microspheres (Figure S2E), thus suggesting that LXR activity selectively affects invasive mechanisms induced by pathogenic bacteria.

Morphological studies using fluorescent phalloidin to stain filamentous actin (F-actin) showed that macrophages incubated with *S.* Typhimurium acquire a round pancake-like shape within minutes after bacterial exposure (Figure 1H), a morphological feature previously associated to inflammatory macrophage polarization (McWhorter et al., 2013). Remarkably, pretreatment with an LXR agonist strongly inhibited the changes in macrophage morphology induced upon *S.* Typhimurium infection without altering the morphology of resting cells (Figure 1H, see quantification in Figure 2E). Moreover, LXR activation also reduced the expression of several pro-inflammatory mediators in infected macrophages (Figure S2F).

Interestingly, expression profiling experiments revealed that interference with bacterial internalization was not mediated by repression of membrane receptors traditionally involved in recognition and/or phagocytosis of bacterial products (Figure S3).

A recent study demonstrated a role for cytosolic nicotinamide adenine dinucleotide (NAD^+) in the control of the organization of the actin cytoskeleton required for the spreading performance and the formation of actin-rich membrane protrusions in activated macrophages (Venter et al., 2014). Based on these observations, we evaluated whether altering NAD^+ levels affects the capability of LXRs to interfere with macrophage morphology and/or internalization of *S.* Typhimurium. In mammalian cells, nicotinamide phosphoribosyltransferase (NAMPT) is the rate-limiting enzyme in the biosynthesis of NAD^+ through the salvage pathway. Incubation with FK866, a specific NAMPT inhibitor, resulted in partial inhibition of the capability of macrophages to internalize *S.* Typhimurium (Figure 2A). Interestingly, activation of the LXR pathway significantly reduced the intracellular levels of NAD^+ (Figure 2B), and addition of exogenous NAD^+

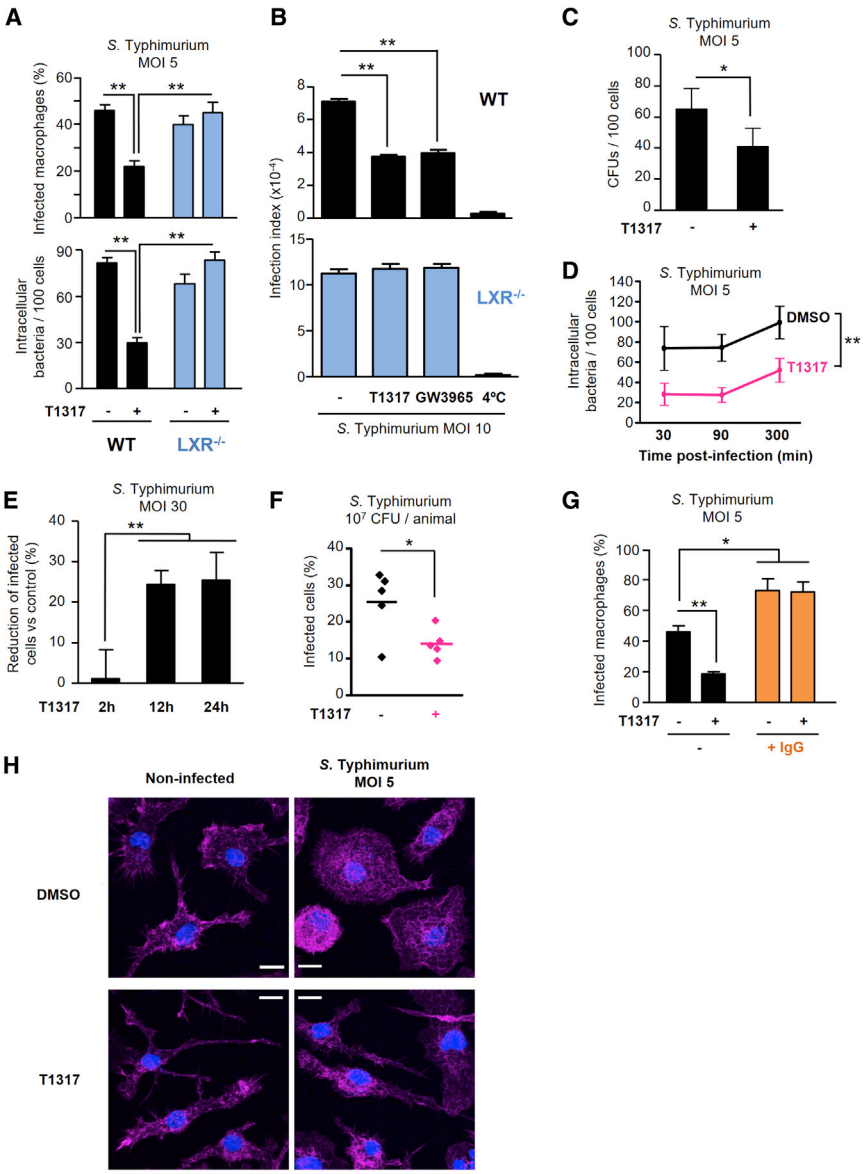

Figure 1. LXR Activation Limits Macrophage Infection by Non-opsonized *S.* Typhimurium

(A) Macrophages from WT (n = 5) or LXR$^{-/-}$ (n = 4) mice treated with the LXR agonist T1317 (1 μM, 24 hr) or DMSO and infected with *S.* Typhimurium (30 min). Analysis of the percentage of infected macrophages (top) and the amount of intracellular bacteria (bottom) by confocal fluorescence microscopy. Data represent mean ± SEM (two-way ANOVA Bonferroni). The dataset in WT cells includes data from Figure 2C.

(B) Analysis of macrophage infection by flow cytometry after incubation with the LXR agonists T1317 or GW3965 (1 μM, 24 hr). Macrophages were infected with *S.* Typhimurium for 30 min at 37°C. As a control, bacterial cell attachment to macrophages (without internalization) was also assessed by carrying out the infection at 4°C. Each experiment was performed in triplicate. Shown is a representative experiment from each genotype (mean ± SD) from n = 5 (WT) or n = 4 (LXR$^{-/-}$) independent experiments (ANOVA Bonferroni).

(C) Quantification of intracellular *S.* Typhimurium burden. The cells were infected for 30 min. Serial dilutions of cell lysates were plated on agar and allowed to grow at 37°C. Bacterial CFUs were counted 24 hr later. Data represent mean ± SEM from n = 3 independent experiments (each including biological duplicates or triplicates) (paired t test).

(D) Confocal fluorescence microscopy evaluating the effects of T1317 on intracellular bacterial burden over time. Data represent mean ± SEM; n = 5 (30 min), n = 7 (90 min), or n = 9 (300 min) (paired t test for each time post-infection).

(E) Macrophages were treated with T1317 for the indicated periods of time, and the inhibitory effects on macrophage infection were evaluated by flow cytometry. Data are expressed as percent reduction in the number of infected cells (versus infection in the absence of T1317) (mean ± SD; n = 5; Kruskal-Wallis Dunn. Similar results were obtained in an independent experiment performed in triplicates.

(F) In vivo infected cells analyzed by confocal microscopy. C57BL/6 male mice were first subjected to an i.p. injection of T1317 (10 mg/kg animal; 24 hr) or vehicle (DMSO in PBS; 24 hr) and then infected i.p. with *S.* Typhimurium (10^7 CFU per animal; 30 min); n = 5 animals/group. Mean bars are indicated (t test).

(G) Bacterial uptake in the presence or absence of opsonizing anti-*Salmonella* LPS IgG. Data represent mean ± SEM (n = 3; Kruskal-Wallis Dunn).

(H) Representative images of infected macrophages stained with phalloidin (F-actin, purple) and DAPI (nuclei, blue) (n = 4). Scale bars, 10 μm.

See also Figures S1 and S2. *p < 0.05, **p < 0.01.

counteracted the ability of the LXR agonist to reduce macrophage infection (Figure 2C), with no effect on the levels of infection in control macrophages (not exposed to LXR agonists). These effects correlated with the observation that in the presence of exogenous NAD$^+$, activation of the LXR pathway did not inhibit morphological changes associated with host cell-pathogen interaction (Figures 2D and 2E). In activated macrophages, changes in macrophage morphology are accompanied by an increase in F-actin-rich dorsal membrane ruffling, with curved or circular protrusions directed upright that precede macropinocytosis (Luo et al., 2014). Interestingly, the LXR agonist interfered with dorsal F-actin accumulation in *Salmonella*-infected cells, and addition of exogenous NAD$^+$ counteracted these effects. Altogether, these observations prompted us to consider whether LXR activation modulates the expression of factors that contribute to NAD$^+$ metabolism as a mechanism protecting macrophages from excessive bacterial internalization.

LXR Agonists Induce the Expression of the NAD Glycohydrolase CD38

In general, NAD$^+$ and its phosphorylated and reduced forms participate as coenzymes in oxidation-reduction reactions

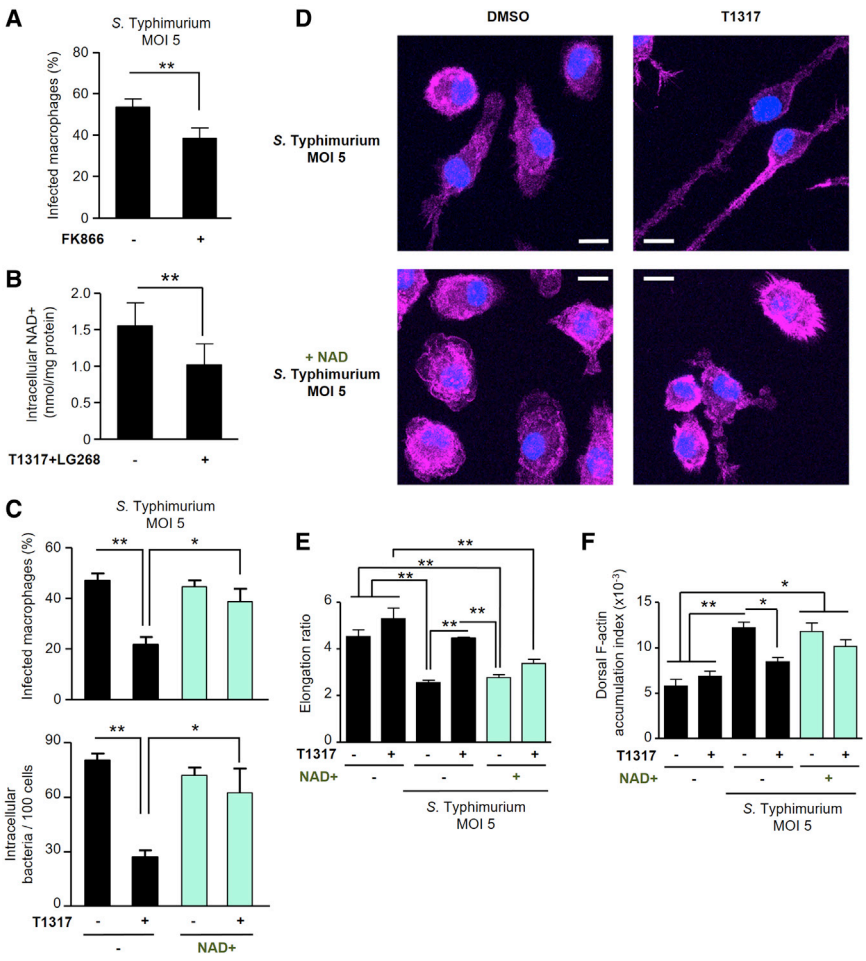

Figure 2. NAD$^+$ Addition Suppresses the Effects of LXR Activation on Macrophage Infection

(A) Confocal fluorescence microscopy analysis of the amount of infected macrophages after treatment with the NAMPT inhibitor FK866 (10 nM) or vehicle for 24 hr. Data represent mean ± SEM (n = 4; paired t test).

(B) Analysis of intracellular NAD$^+$ levels with a NAD cycling assay. The cells were pre-treated with agonists for the LXR-RXR heterodimer, T1317 and LG268 (1 μM each), or vehicle (DMSO) for 24 hr. Data represent mean ± SEM (n = 6; paired t test).

(C) Effects of exogenous addition of NAD$^+$ on macrophage infection. The cells were pretreated with T1317 (1 μM, 24 hr) or DMSO and then incubated with NAD (1 mM) for 2 hr before the infection. Results of confocal microscopy studies are shown. Data represent mean ± SEM (n = 4; two-way ANOVA Bonferroni). The data from WT cells are also included as part of the WT dataset in Figure 1A.

(D) Effects of NAD$^+$ on *S.* Typhimurium-induced changes in macrophage morphology; scale bars, 10 μm. Representative images; n = 4.

(E and F) Cell elongation ratio (E) and dorsal F-actin accumulation index (F). Data represent mean ± SEM (n = 4; ANOVA Bonferroni).

*p < 0.05, **p < 0.01.

without net consumption of intracellular NAD. In contrast, NAD$^+$ is consumed as a substrate by enzymatic activities that mediate protein lysine deacylation and ADP-ribose transfer or synthesis (Belenky et al., 2007). To assess if LXR activation modulates the expression of enzymes that participate in NAD$^+$ biosynthesis or consumption, we analyzed expression-profiling data obtained from macrophages stimulated with an LXR agonist (Figure 3A). The expression of most of the genes evaluated, including *Nampt*, was not altered upon LXR activation. However, selective induction of *Cd38* was observed in cells treated with the LXR agonist. CD38 is a type II transmembrane glycoprotein that catalyzes the conversion of NAD$^+$ into nicotinamide, adenosine diphosphate-ribose (ADPR), and cyclic ADPR (cADPR) (Chini, 2009) and is thus a major regulator of cellular levels of NAD$^+$ (Aksoy et al., 2006). Induction of CD38 upon LXR activation was confirmed by qPCR (Figures 3B and 3C) and western blotting (Figure 3D). It is noteworthy that the basal levels of *Cd38* expression were not significantly reduced in LXR-deficient cells, as it is the case for previously identified LXR target genes (e.g., *Abca1*, *Abcg1*, and *Srebp1c*; Wagner et al., 2003); however, *Cd38* induction by the LXR agonist was LXR dependent and LXR specific (Figure 3B). *Cd38* expression was also upregulated in response to a synthetic agonist for RXR, LG268 (Figure 3B), and combined treatment with agonists for LXR and RXR synergistically upregulated CD38 mRNA and protein expression (Figures 3B, 3E, and 3F) in an LXR-dependent manner, with both LXRα and LXRβ contributing to *Cd38* induction (Figure 3F). Moreover, these effects translated into increased CD38 protein levels at the cell surface (Figure 3G) and augmented cellular NADase activity (Figures 3H–3J). The changes in NADase activity were completely abolished in either LXR$^{-/-}$ or CD38$^{-/-}$ macrophages (Figures 3I and 3J), which correlated with the fact that LXR/RXR agonists significantly downregulate intracellular NAD$^+$ levels in wild-type (WT) cells (Figure 2B), but not in CD38-deficient cells (Figure 3K). Taken together, these results indicate that CD38 mediates the increase in NADase activity and the reduction in intracellular NAD levels upon pharmacological activation of the LXR pathway.

A putative LXR response element (LXRE) was identified in an enhancer ~2 kb upstream of the transcription initiation site, which is fully conserved at least in mouse and rat. A fragment containing the potential LXRE, hereafter named *Cd38* enhancer (*Cd38*enh), was cloned in a pGL3-promoter vector (pGL3-*Cd38*enh), and its activity was characterized in COS-7 cells. Co-transfection of LXRα and RXRα resulted in maximal induction of promoter activity in response to a combination of LXR and RXR agonists (Figure S4). Significant loss of activity was observed after mutation of the potential LXRE in the *Cd38*enh region, which suggests that the site identified here represents a bona fide LXRE (Figure 3L).

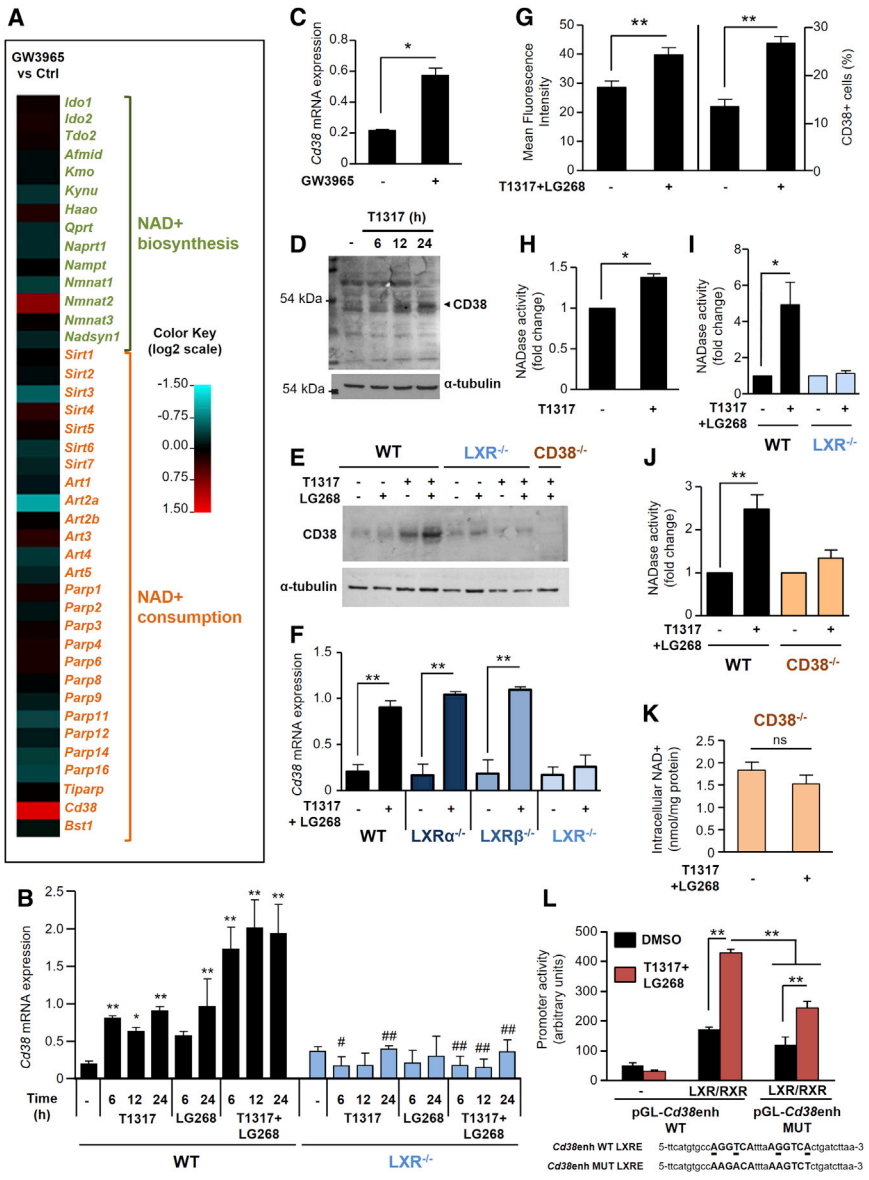

Figure 3. LXR Activation Induces the Expression of the Multifunctional Enzyme CD38

(A) Expression profiling from macrophages treated with GW3965 (2 μM) or DMSO for 18 hr. Heatmap representing average fold expression values (log2 scale) of genes involved in net NAD^+ synthesis or consumption in GW3965-treated cells over DMSO-treated cells (n = 2).

(B and C) qPCR analysis of *Cd38* expression in WT and LXR-deficient macrophages stimulated with LXR agonists T1317 or GW3965 and/or the RXR agonist LG268 (1 μM each). Data represent mean ± SEM (n = 4 with two-way ANOVA Bonferroni in B; n = 3 with t test [with Welch's correction] in C). In (B), *p < 0.05, **p < 0.01 vs control cells from the same genotype; #p < 0.05, ##p < 0.01 vs the same treatment in WT cells.

(D and E) Western blot analysis of CD38 protein expression in WT (D and E) and LXR-deficient and CD38-deficient macrophages (E).

(F) qPCR analysis in macrophages WT or deficient in LXRα ($LXR\alpha^{-/-}$), LXRβ ($LXR\beta^{-/-}$), or both isoforms ($LXR^{-/-}$). Data represent mean ± SEM (n = 4; t test for each genotype).

(G) Flow cytometry analysis of the surface expression of CD38. Data represent mean ± SEM (n = 6; t test).

(H–J) Fluorimetric determination of intracellular NADase activity in WT (H–J), LXR-deficient (I), and CD38-deficient macrophages (J). Data represent mean ± SEM (n = 4 in H, n = 3 in I, and n = 5 in J; Mann-Whitney *U* Wilcoxon test for each genotype).

(K) Intracellular NAD^+ levels in CD38-deficient macrophages. Data represent mean ± SEM (n = 6; paired t test).

(L) Luciferase reporter studies in COS7 cells co-transfected with a WT *Cd38* enhancer-luciferase construct (pGL-*Cd38*enh WT) or a construct containing a mutated LXRE (pGL-*Cd38*enh MUT), as well as plasmids overexpressing LXRα and RXRα or an empty vector. Transfected cells were stimulated for 18 hr with either vehicle (DMSO) or LXR-RXR agonists. Data represent mean ± SEM (n = 3, left; n = 6, middle; and n = 4, right; ANOVA Bonferroni comparing transfections with LXR/RXR coexpression).

See also Figure S4. *p < 0.05, **p < 0.01.

Cooperative Effects of LXRs and Inflammatory Signals on CD38 Expression and NADase Activity

Interestingly, infection by *S.* Typhimurium strongly induced macrophage expression of *Cd38* (Figure 4A). In agreement with previous observations (Musso et al., 2001; Iqbal and Zaidi, 2006; Lee et al., 2012), increased expression of *Cd38* was observed upon prolonged stimulation with IFN-γ, lipopolysaccharide (LPS), or tumor necrosis factor alpha (TNF-α) (Figures 4B and S5A–S5C). In contrast, *Cd38* was not upregulated in macrophages alternatively activated by interleukin 4 (IL-4), IL-10, or transforming growth factor beta (TGF-β) (Figure 4C), despite the fact that these cytokines did induce specific target genes in macrophages (Figures S5D–S5F). In line with increased *Cd38* expression in classically activated macrophages, inflammatory mediators reduced intracellular NAD^+ levels in a CD38-dependent manner (Figure 4D). However, despite the ability of CD38 to alter intracellular NAD^+ levels, early ROS production in response to inflammatory signaling was CD38 independent (Figure 4E).

These studies also led to the unexpected observation that functional LXR expression was required for full induction of *Cd38* by inflammatory signals and that combined activation of inflammatory signaling and the LXR pathway cooperated synergistically to upregulate *Cd38* expression (Figures 4A, 4B, and S5A–S5C) and NADase activity (Figures 4F and S5G). Sequence analysis of the *Cd38*enh region containing the LXRE revealed the presence of two nuclear factor κB (NF-κB) binding sites, an interferon-stimulated response element (ISRE), and an AP-1 site in the proximity of the LXRE. Raw264.7 macrophages that stably express human LXRα were cotransfected with the *Cd38*enh-luciferase reporter and a plasmid overexpressing RXRα. In these studies,

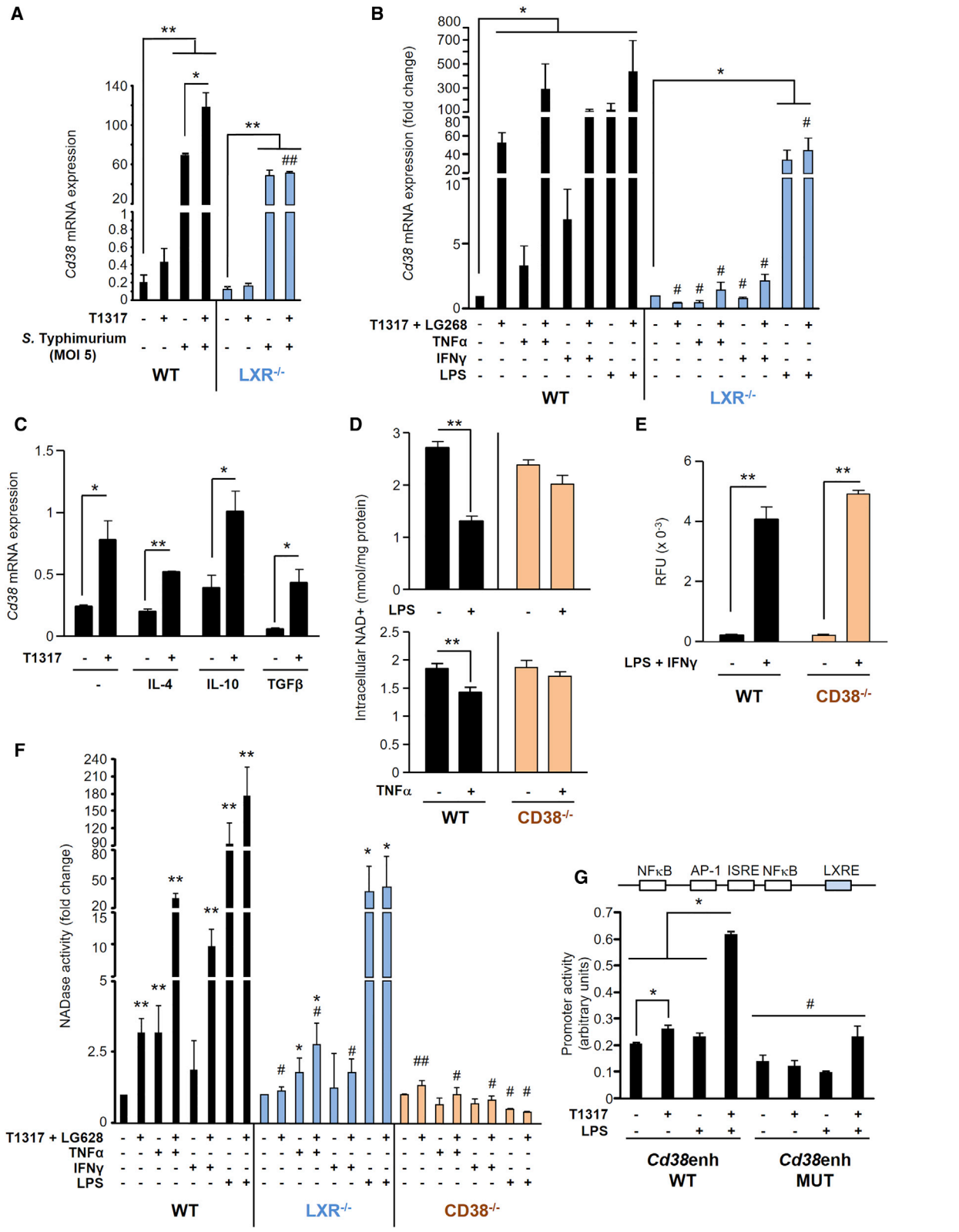

(legend on next page)

cooperation of the LXR pathway with LPS signaling occurred at the transcriptional level, and these effects were abolished when the cells were transfected with the mutant LXRE (Figure 4G).

CD38 Mediates the Protective Effects of LXR Agonists on Macrophage Infection

We next compared the capability of an LXR agonist to protect WT and CD38-deficient macrophages from infection by *S.* Typhimurium. Importantly, the lack of functional expression of CD38 inhibited the capability of the LXR agonist to reduce the amount of infected macrophages and intracellular bacteria (Figure 5A), effects that were similar to those obtained upon addition of exogenous NAD^+ in WT cells (Figure 2C). Moreover, activation of macrophages by IFN-γ has been shown to regulate negatively their capability to internalize non-opsonized bacteria in certain models of infection (Wang et al., 2014; Sun and Metzger, 2008). Interestingly, in our studies, prolonged stimulation with IFN-γ resulted in decreased infection by non-opsonized *Salmonella* cells in a CD38-dependent manner (Figure 5B). Taken together, these results suggest that induction of macrophage CD38 expression represents a strategy to limit infection of macrophages by live *Salmonella* cells.

We also determined the inflammatory response to infection in CD38-deficient macrophages (Figure 5C). To our surprise, the levels of induction of several cytokines were significantly lower in CD38-deficient cells as compared to WT cells. However, for most of the genes examined, LXR agonists were able to repress inflammatory gene expression in cells lacking functional CD38. These data suggest that CD38 selectively facilitates protection against invasive bacterial cell entry but does not contribute broadly to the LXR-mediated anti-inflammatory response in vitro.

Intrinsic to its NADase activity, CD38 mediates the synthesis of ADPR, cADPR, and nicotinic acid adenine dinucleotide phosphate (NAADP), which are Ca^{2+} mobilizing compounds (Musso et al., 2001). Video microscopic measurements from fura-2-AM-loaded cells showed higher basal levels of cytosolic Ca^{2+} in WT macrophages than in LXR-deficient cells (Figure 5D, top). However, Ca^{2+} storage in the endoplasmic reticulum (ER) was not depleted by prolonged treatment with the LXR agonist or by addition of exogenous NAD^+, as shown in experiments in which the cells were acutely stimulated with the sarco-ER Ca^{2+} ATPase inhibitor thapsigargin (Figure 5D, bottom). Altogether, these results suggest that induction of the LXR-CD38 circuit has no substantial long-term impact on Ca^{2+} depletion from the ER in macrophages. In addition, incubation of WT cells with *S.* Typhimurium did not lead to significant cytosolic Ca^{2+} changes in either the presence or absence of an LXR agonist (Figure 5E), and treatment with 8-bromo-cADPR, an analog of cADPR that blocks Ca^{2+} release mediated by ryanodine-receptor-gated stores, did not affect the capability of LXRs to inhibit macrophage infection (Figure 5F). Based on all of these observations, we conclude it is the CD38-dependent reduction in NAD^+ levels (a consequence of its strong NADase activity) and not the concomitant generation of potential Ca^{2+}-mobilizing second messengers that best explains the protective effects on macrophage infection induced by the LXR-CD38 axis. Importantly, lack of functional CD38 expression counteracted the capability of an LXR agonist to inhibit changes in F-actin redistribution and cell morphology associated with bacterial infection (Figures 5G–5I).

An Endogenous Pathway Can Activate the LXR-CD38 Axis during *Salmonella* Infection

Endogenous LXR ligands are generated enzymatically from intermediates of the cholesterol biosynthetic pathway or by oxidation of cholesterol by sterol hydroxylases (Spann et al., 2012). Interestingly, infection of macrophages with *S.* Typhimurium resulted in reduced expression of several enzymes involved in cholesterol biosynthesis but a selective prominent increase in the expression of cholesterol 25-hydroxylase (*Ch25h*), which mediates cholesterol oxidation to 25-hydroxycholesterol (25-HC) (Figure 6A). 25-HC is a relatively weak LXR activator that is able to induce LXR-mediated transcriptional activity at high doses (Lala et al., 1997; Janowski et al., 1999). In our studies, micromolar doses of 25-HC induced the expression of *Cd38*, either alone or in synergy with IFN-γ (Figure 6B), and reduced macrophage infection in an LXR- and CD38-dependent manner (Figures 6C and 6D). 25-HC can modulate inflammatory responses both positively and negatively in different settings (Reboldi et al., 2014; Gold et al., 2014). In macrophages infected with *Salmonella*, 25-HC exerted dose-dependent repression of inflammatory genes (Figure 6E). However, these actions were independent of the LXR-CD38 pathway (Figure 6E), in contrast to

Figure 4. Synergistic Induction of *Cd38* by Inflammatory Signals and LXR Activation

(A–C) qPCR analysis of *Cd38* expression in WT (A–C) or LXR-deficient macrophages (A and B) in response to one or more stimuli: *S.* Typhimurium (MOI 5, 8 hr), LXR agonist T1317 (1 μM, 8 hr in A or 24 hr in B), RXR agonist LG268 (1 μM, 24 hr), TNF-α (20 ng/mL, 24 hr), IFN-γ (5 ng/mL, 24 hr), LPS (100 ng/mL, 24 hr), IL-4 (20 ng/mL, 18 hr), IL-10 (10 ng/mL, 18 hr), and TGF-β (2 ng/mL, 18 hr). Data represent mean ± SEM (n = 3). In (A) and (B), #p < 0.05, ##p < 0.01 versus the same treatment in WT cells. Statistical analysis was performed with a two-way ANOVA Bonferroni (A), Kruskal Wallis followed by Mann-Whitney *U* test for paired comparisons (B), or t test (C).

(D) Intracellular NAD^+ levels in WT and CD38-deficient macrophages stimulated or not with LPS (100 ng/mL) (top) or TNF-α (20 ng/mL) (bottom) for 24 hr. Data represent mean ± SEM; n = 7 (WT, top), n = 3 ($CD38^{-/-}$, top), n = 10 (WT, bottom), and n = 6 ($CD38^{-/-}$, bottom) (t test).

(E) Fluorimetric analysis of intracellular ROS production in response to LPS (100 ng/mL) and IFN-γ (5 ng/mL) (6 hr) in WT and CD38-deficient cells. Data represent mean ± SD (representative experiment of n = 4, with each experiment using biologically distinct triplicates).

(F) Intracellular NADase activity. Data represent mean ± SEM; n = 5 (WT) and n = 3 ($LXR^{-/-}$, $CD38^{-/-}$) (each experiment performed with cells pooled from at least two mice). Statistical analysis was performed using a Kruskal-Wallis test. *p < 0.05, **p < 0.01 vs control cells from the same genotype; #p < 0.05, ##p < 0.01 vs same treatment in WT cells.

(G) Luciferase reporter studies in Raw264.7 macrophages stably transfected with LXRα and transiently cotransfected with a reporter plasmid containing the *Cd38* enhancer with WT LXRE (*Cd38*enh WT) or with mutated LXRE (*Cd38*enh MUT), as well as a plasmid overexpressing RXRα. Transfected cells were stimulated for 24 hr with vehicle (DMSO), T1317 (1 μM), LPS (100 ng/mL), or a combination of both. Data represent mean ± SEM (n = 4). #p < 0.05 versus the same treatment in cells transfected with the WT construct (Kruskal-Wallis).

See also Figure S5. *p < 0.05, **p < 0.01.

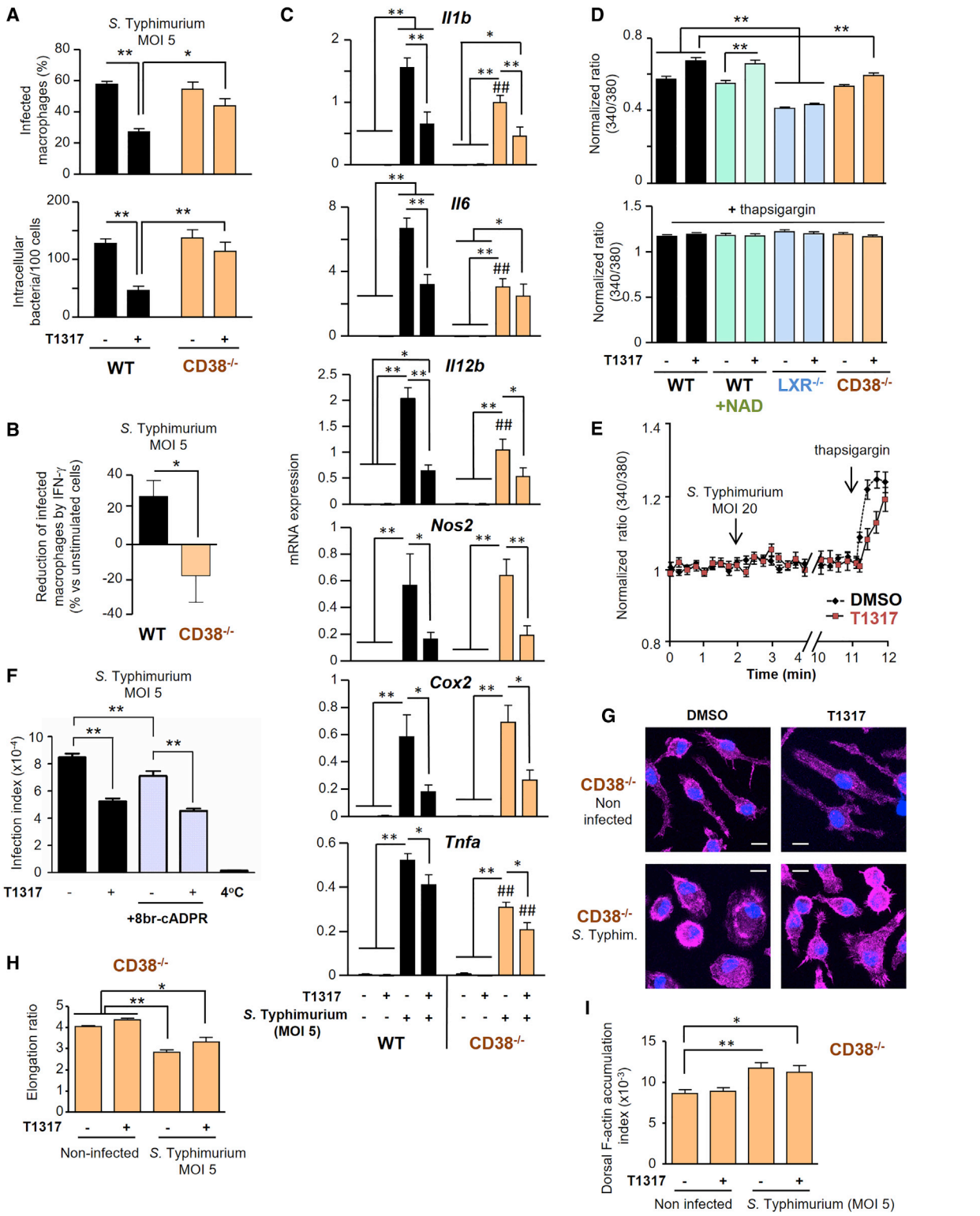

Figure 5. CD38 Mediates the Protective Effects of LXR Agonists on Macrophage Infection

(A) Effects of the LXR agonist T1317 on the percentage of infected cells (top) and the amount of intracellular bacteria (bottom) in WT and CD38-deficient macrophages, as assessed by confocal fluorescence microscopy. Data represent mean ± SEM (n = 4; two-way ANOVA Bonferroni).

(legend continued on next page)

the role in macrophage bacterial infection. Altogether, these observations suggest that induction of CH25H during the host innate response against *Salmonella* may provide local endogenous LXR agonists that limit subsequent macrophage infection through the LXR-CD38 circuit and, in parallel, activate mechanisms that are independent of LXRs to further keep inflammatory responses under control.

Pharmacological Treatment with a Synthetic LXR Agonist Ameliorates the Clinical Signs Associated with Bacterial Infection In Vivo

Based on the findings described throughout this work, we next analyzed whether pharmacological treatment with a synthetic agonist has protective effects on *Salmonella* infection in vivo. Mice were administered either vehicle or the LXR agonist T1317 daily during the course of a lethal infection with *S.* Thyphimurium and monitored for the first 5 days post-infection. Remarkably, pharmacological LXR activation resulted in a significant decrease in body mass loss and in the severity of the clinical score during the course of infection (Figures 7A and 7B). The ameliorating effects of the agonist were abolished in animals deficient in LXRs (Figures 7C and 7D) or CD38 (Figures 7E and 7F). In LXR$^{-/-}$ mice, in fact, treatment with T1317 accelerated the loss of weight associated to infection. Moreover, in WT mice, but not in CD38$^{-/-}$ mice, the agonist decreased the infection index of splenocytes 4 days after the start of infection (Figures 7G and 7H) as well as the expression of several markers of inflammation in the liver and spleen (Figure S6), suggesting that pharmacological activation of LXRs inhibited the capability of orally administered *Salmonella* to disseminate and infect distant organs.

To evaluate the specific contribution of bone-marrow-derived CD38-expressing cells, we analyzed the response to infection in mice that had been sub-lethally irradiated and transplanted with either WT or CD38-deficient bone marrow. Interestingly, activation of the LXR pathway did not reduce the loss of body weight and other clinical signs associated with infection in mice reconstituted with CD38$^{-/-}$ bone marrow, in contrast to the ameliorating effects observed in mice transplanted with WT bone marrow (Figures 7I–7J). In correlation with these observations, treatment with the LXR agonist significantly inhibited the infection index of splenocytes (Figure 7K) and the expression of several inflammatory genes in WT, but not CD38-deficient, bone marrow recipients (Figure S7). Collectively, these results suggest that CD38 induction in bone-marrow-derived cells is an important mediator of the ameliorating actions of the LXR pathway in *Salmonella* infection.

DISCUSSION

In this study, we have identified a previously unappreciated strategy to inhibit the potential of *S.* Typhimurium to infect host macrophages based on pharmacological targeting of the LXR pathway. A key finding of our work is the mechanism that accounts for these protective effects, which involves transcriptional upregulation of the multifunctional enzyme CD38. Interestingly, LXR activation did not interfere with phagocytosis of IgG-opsonized bacteria, suggesting that the protective effects of LXR agonists do not interfere with bacterial clearance through Fcγ receptors once the adaptive immune system has generated opsonizing antibodies against the pathogen.

A role for CD38 in the host response against bacteria has been previously proposed based on increased susceptibility of CD38-deficient mice to other bacterial strains, in correlation with defects in immune cell infiltration to sites of infection (Partida-Sánchez et al., 2001; Lischke et al., 2013) or with defective polarization of Th1 immune responses (Viegas et al., 2007). In this work, we describe a previously unrecognized function of CD38 in mediating macrophage protection from invasive bacterial infection. The major enzymatic activity of CD38 is considered to be its NADase activity, as it hydrolyzes 100 molecules of NAD^+ to generate 1 molecule of cADPR (Aksoy et al., 2006). In the model we propose here, LXR activation reduces NAD^+ levels as a consequence of elevated CD38 expression, resulting in cytoskeletal changes that interfere with membrane ruffling and/or other mechanisms subverted by invasive bacterial strains. Consistent with this model, addition of NAD^+ reverted the changes in cell morphology and dorsal F-actin accumulation in macrophages and rescued the capability of *S.* Typhimurium to infect macrophages in the presence of an LXR agonist. The virulence of invasive *Salmonella* strains correlates with their capability to induce extensive cell membrane ruffling and macropinocytosis and enter inside macrophages via ''spacious phagosomes'' (Kiama et al., 2006; Alpuche-Aranda et al., 1995). Among the effectors secreted by *S.* Typhimurium, cell invasion protein A increases the actin polymerization rate (Lilic et al., 2003) and Salmonella outer protein E enhances the activity of host cell Rho family GTPases involved

(B) Treatment with IFN-γ (5 ng/mL, 24 hr) reduced the infection in WT, but not CD38-deficient, macrophages, as assessed by confocal microscopy. Data represent mean ± SEM (n = 3; Mann-Whitney Wilcoxon).

(C) Repressive effects of T1317 on proinflammatory gene expression in WT and CD38-deficient macrophages (qPCR analysis). Data represent mean ± SEM (n = 5; two-way ANOVA Bonferroni). ##$p < 0.01$ vs the same treatment in WT cells.

(D and E) Video microscopic analysis of cytosolic Ca^{2+} levels in WT (D and E), LXR-deficient (D), and CD38-deficient (D) macrophages loaded with fura-2 AM. Prior to the analysis, the cells were stimulated with T1317 (1 μM, 24 hr) or vehicle (DMSO) with or without exogenous addition of NAD^+ (1 mM) for the last 2 hr of treatment. In (D, bottom), changes in cytosolic Ca^{2+} levels after inducing Ca^{2+} mobilization from the ER by thapsigargin (1 μM). In (D), data represent mean ± SEM (pooled data from three independent experiments; Kruskal Wallis). (E) Representative experiment showing that infection by *S.* Typhimurium (MOI 20) did not result in changes in cytosolic Ca^{2+} levels in cells previously stimulated or not with T1317. As a control, the response to thapsigargin was also evaluated; data represent mean ± SD (n = 3, each experiment performed in triplicates). Similar results were obtained using MOIs 5–10.

(F) Treatment with 8br-cADPR (20 μM, 2 hr) does not impair the capability of T1317 to inhibit macrophage infection, as assessed by flow cytometry studies of macrophage infection. Data represent mean ± SEM (n = 3; ANOVA Bonferroni).

(G–I) Morphological analysis by confocal fluorescence microscopy of CD38-deficient macrophages. Representative images (scale bars, 10 μm) (G), cell elongation ratio (H), and dorsal F-actin accumulation (I). Data represent mean ± SEM (n = 3; ANOVA Bonferroni).

*$p < 0.05$, **$p < 0.01$.

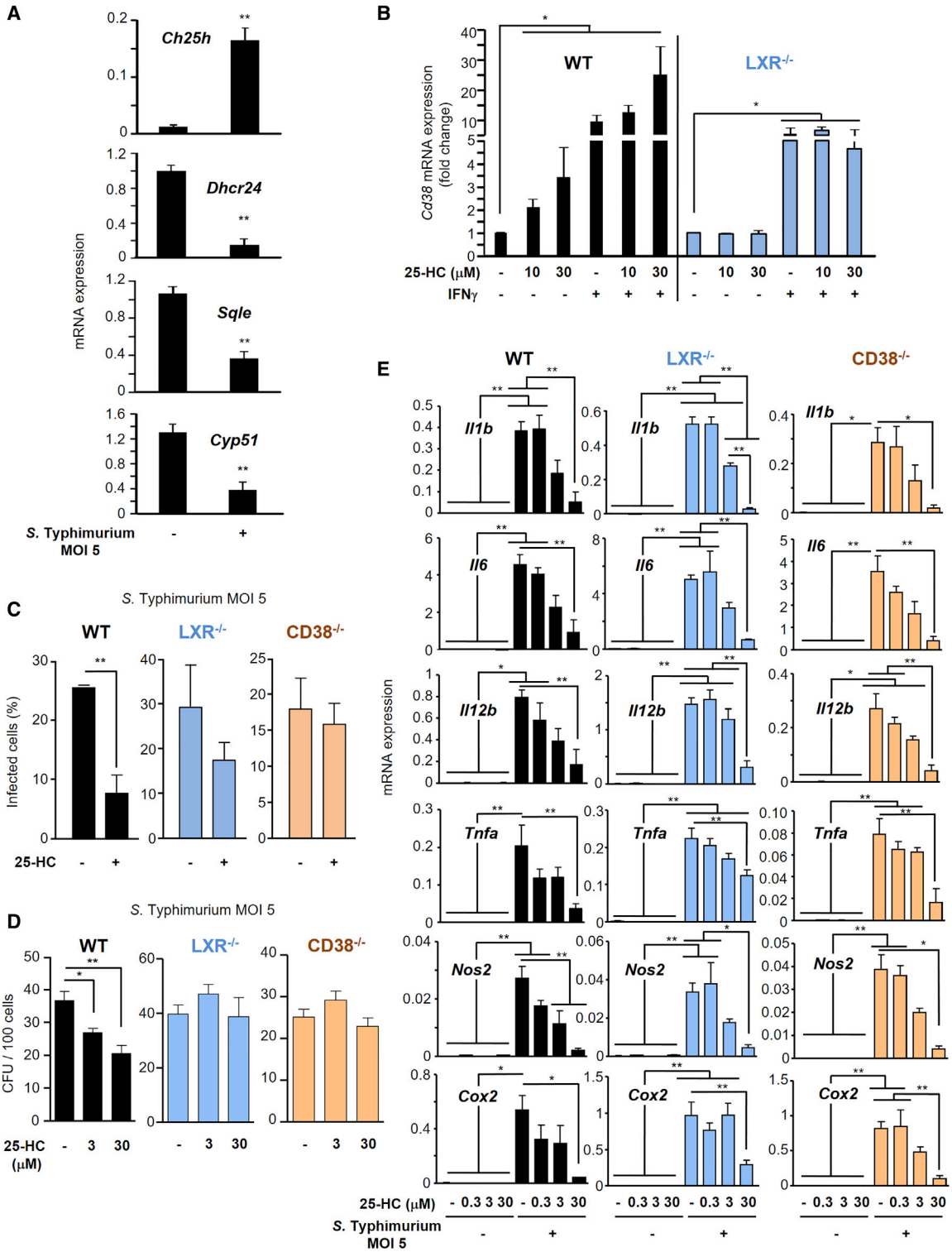

Figure 6. *Salmonella* Infection Induces the Expression of *Ch25h* in Macrophages

(A) Effects of *Salmonella* infection on the relative mRNA levels of several enzymes involved in cholesterol and oxysterol biosynthesis. Macrophages were infected with *S.* Typhimurium for 30 min, and gene expression was evaluated by qPCR 8 hr post-infection. Mean ± SEM (n = 3; t test). *Cyp51*, sterol 14α-demethylase; *Dhcr24*, 24-dehydrocholesterol reductase; *Sqle*, squalene epoxidase.

(legend continued on next page)

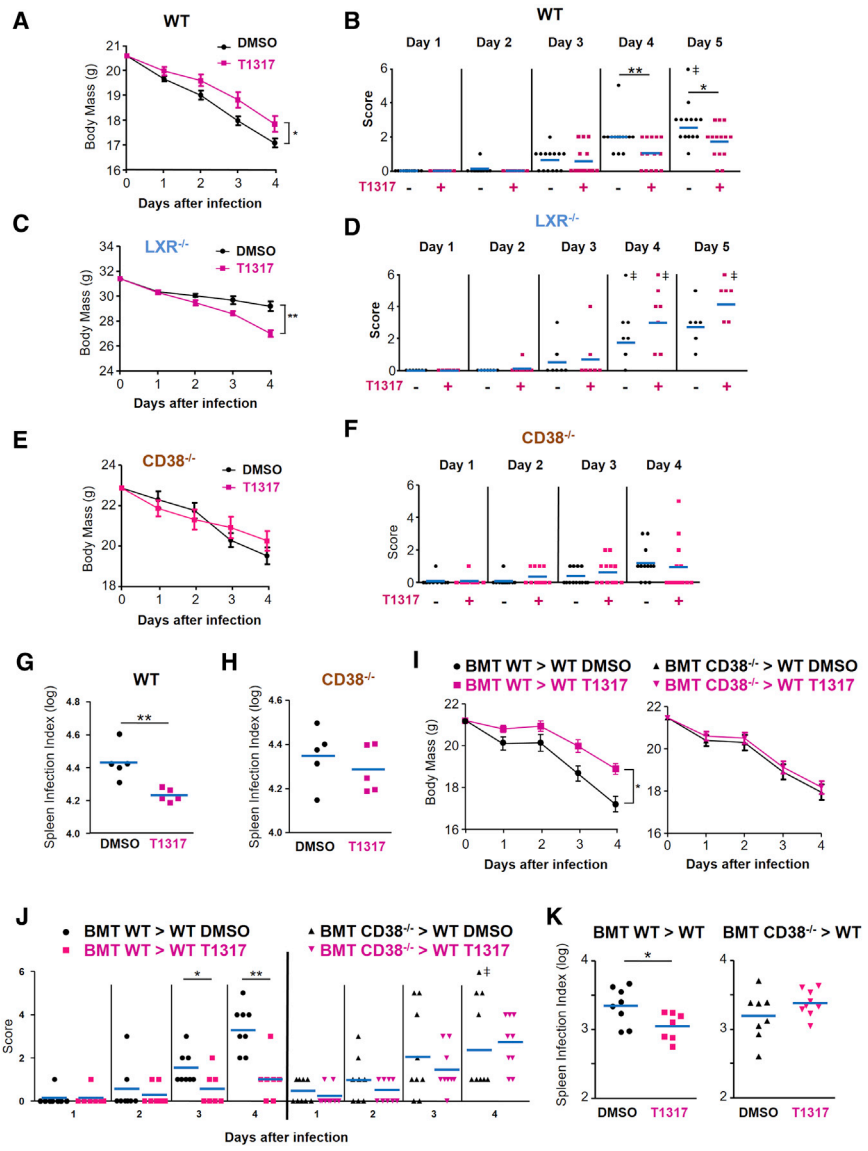

Figure 7. Pharmacological Treatment with a Synthetic LXR Agonist Ameliorates the Clinical Signs Associated with *Salmonella* Infection in a CD38-Dependent Manner

WT (A and B), LXR-deficient (C and D), or CD38-deficient (E and F) female mice were infected by oral gavage with *S.* Typhimurium (10^7 CFU per animal). The animals were daily administered by i.p. injection either vehicle (DMSO in physiologic saline, black circles) or the LXR ligand T1317 (15 mg/kg animal dissolved in physiologic saline, magenta squares), starting 24 hr before the infection; n = 14 (WT), n = 7 ($LXR^{-/-}$), and n = 13 ($CD38^{-/-}$) mice per group.

(A, C, and E) The weight of each mouse was measured daily before and after the infection. The graphics represent estimated marginal means of mass (±SEM) during the first 4 days post-infection. Statistical analysis was performed using repeated-measures two-way ANCOVA after adjusting for mass at the time of infection.

(B, D, and F) Development of clinical signs during the first few days of infection. For each mouse, a score was calculated based on the presence of clinical signs (one point for each sign): >15% weight loss, severe hunched position, ruffled fur, watery eyes, or slow movement. Dead animals (ǂ) were assigned a score of 6. Horizontal bars represent mean values in the live population (Mann-Whitney *U*).

(G and H) WT (G) or CD38-deficient (H) female mice were orally infected with RFP-expressing *S.* Typhimurium (10^7 CFU per animal) and treated with vehicle or an LXR agonist as described above. The infection index in splenocytes after 4 days of infection was determined by flow cytometry (log values); n = 5 mice per group (t test).

(I–K) Sub-lethally irradiated WT female mice were subjected to bone marrow transplantation (3 × 10^6 bone marrow cells per animal) from either WT (BMT WT > WT) or CD38-deficient female donors (BMT $CD38^{-/-}$ > WT). Two months after transplantation, the animals were infected with RFP-expressing *S.* Typhimurium (10^7 CFU). Bacterial infection and administration of LXR agonist or vehicle was performed as described above. Body weight (I) and severity score (J) were registered during 4 days post-infection. The infection index in splenocytes was evaluated by flow cytometry (K); n = 7–9 mice per group. Estimated marginal means of mass (± SEM) and repeated-measures two-way ANCOVA after adjusting for mass at the time of infection (I), Mann-Whitney *U* (J), or t test (K). In (J)–(K), blue horizontal bars indicate mean values.

See also Figures S6 and S7. *p < 0.05, **p < 0.01.

in the regulation of the cytoskeleton (Hardt et al., 1998). Moreover, NAD^+ is used as a cofactor to sustain the glycolytic activity in macrophages and generate ATP for polymerization of F-actin filaments and may also modulate actin dynamics through several other mechanisms (Yin et al., 2012; Venter et al., 2014).

(B) *Cd38* mRNA expression was evaluated by qPCR upon treatment of WT or LXR-deficient macrophages with the indicated doses of 25-HC in the presence or absence of IFN-γ (5 ng/mL). Mean ± SEM (n = 3; Kruskal-Wallis).

(C) Confocal microscopy studies indicating that incubation with 25-HC (30 μM) reduced infection by *S.* Typhimurium in WT, but not LXR- or CD38-deficient, macrophages. Data represent mean ± SEM (n = 3; t test).

(D) Quantification of viable intracellular *S.* Typhimurium. Macrophages from WT (left), LXR-deficient (middle), or CD38-deficient (right) were treated with 25-HC (3–30 μM) or vehicle (ethanol) for 18 hr and then infected with *S.* Typhimurium for 30 min. Quantification of intracellular bacterial CFUs after plating serial dilutions of cell lysates on agar. Data represent mean ± SEM (n = 6; ANOVA Bonferroni).

(E) 25-HC modulates inflammatory gene expression independently of LXR and CD38. Macrophages were treated with 25-HC (0.3–30 μM) 18 hr before infection with *S.* Typhimurium. Inflammatory gene expression was determined by qPCR 6 hr post-infection. Data represent mean ± SEM (n = 4; ANOVA Bonferroni).

*p < 0.05, **p < 0.01.

We have identified a functional LXRE that conferred LXR/RXR agonist responsiveness to a *Cd38* enhancer-directed luciferase construct. Interestingly, CD38 expression can be also induced by other members of the nuclear receptor family, including retinoic acid receptor alpha (Drach et al., 1994) and peroxisome proliferator-activated receptor gamma (Song et al., 2012). Although we cannot discard possible cooperation between other RXR heterodimeric partners and LXRs, the induction of macrophage CD38 by LXR/RXR agonists and the protective mechanism uncovered here depends on functional LXR expression, suggesting that these effects are mediated directly by LXR-RXR heterodimers.

Another major insight from this report is that cooperative actions between LXRs and inflammatory signals translate into synergistic induction of CD38 expression and its NADase activity. Our reporter studies suggest that these effects occur through combined actions at the transcriptional level, which contrasts with general mutually repressive activities between LXRs and LPS or IFN-γ (Castrillo et al., 2003; Ghisletti et al., 2007; Pascual-García et al., 2013). Our results support the notion that such cooperative regulation of macrophage CD38-dependent NADase activity represents a protective mechanism to control excessive internalization of live bacterial cells. This mechanism may be induced endogenously to some extent through induction of CH25H during infection and subsequent production of the oxysterol 25-HC. Micromolar doses of 25-HC resulted in CD38 upregulation and protection from macrophage infection in an LXR- and CD38-dependent manner, raising the possibility that, within infected tissues, intracellular or locally secreted 25-HC levels that reach the threshold to activate the LXR pathway, in combination with inflammatory mediators, contribute to limit intracellular macrophage infection.

Importantly, pharmacological treatment with a high-affinity LXR agonist ameliorated the levels of infection in the spleen and the clinical signs of disease after oral administration of *S.* Typhimurium in a CD38-dependent manner. Once they have infected intestinal epithelial cells, *Salmonella* cells continue to disseminate to other organs and their intracellular life within macrophages is essential for dissemination. We therefore hypothesize that pharmacological activation of the LXR-CD38 circuit, most probably enhanced by mediators in the inflammatory milieu, protects uninfected macrophages from posterior infection, therefore restraining the capability of *Salmonella* cells to disseminate throughout the body. Moreover, the LXR agonist also exerts anti-inflammatory actions that contribute to amelioration of the severity score of disease. Interestingly, despite the fact that LXR agonists repress macrophage inflammatory gene expression independently of CD38 in vitro, the induction of a number of inflammatory mediators in both the spleen and the liver of *Salmonella*-infected animals was downregulated by the LXR agonist in WT, but not CD38-deficient, mice. We interpret that two mechanisms affecting the extent of inflammation may be operating simultaneously in vivo: on one hand, LXR may repress the inflammatory response independently of CD38, and, on the other hand, the LXR-CD38 axis protects macrophages from infection, thus reducing bacterial dissemination to other organs and indirectly contributing to downregulated inflammation. Beyond these considerations, we cannot discard the contribution of other mechanisms regulated by LXRs, such as induction of SPα/AIM, a protein that protects macrophages from bacterial-induced cell death (Joseph et al., 2004; Valledor et al., 2004) and regulates autophagy during mycobacterial infection (Sanjurjo et al., 2015). Importantly, our bone marrow transplantation studies provide evidence that the expression of CD38 specifically in bone-marrow-derived cells is important for the LXR-mediated effects described here, including the reduction in the levels of splenocyte infection, the extent of inflammation, and other clinical signs associated with *Salmonella* infection. Our studies, however, do not exclude that CD38 expression in bone-marrow-derived cells other than macrophages (e.g., neutrophils) contributes to the observed effects of the LXR agonist in vivo. Indeed, the concerted activities of CD38 seem to favor the extracellular permanence of invasive bacterial strains, as suggested here, and the chemotaxis of neutrophils to sites of infection (Partida-Sánchez et al., 2001), which may, in parallel, promote extracellular bacterial killing and limit macrophage-mediated dissemination. In consideration of evolving antimicrobial resistance in certain parts of the world, this work strengthens the relevance of LXR agonists or drugs that potentiate CD38 NADase activity as potential therapeutic strategies in host-directed therapy against infections that use the macrophage as a niche for replication.

EXPERIMENTAL PROCEDURES

See Supplemental Experimental Procedures for more information.

Animal Strains

All the protocols requiring animal manipulation have been approved by the ethical committee from Parc Científic de Barcelona, University of Barcelona, Mayo Clinic and Institut Pasteur in Montevideo.

Cell Cultures

Bone-marrow-derived macrophages were obtained from bone marrow precursors differentiated for 6–7 days in DMEM (PAA Laboratories) supplemented with 20% heat-inactivated fetal bovine serum (FBS) (PAA) and 30% L-cell conditioned medium. Both female and male mice were used indistinctively for generation of primary macrophages. Raw264.7 macrophages and COS-7 (ATCC) cells were grown in DMEM 10% heat-inactivated FBS.

In Vitro Infection

Macrophages were plated in cell culture plates containing DMEM 10% FBS and infected with *S.* Typhimurium or *E. coli* for 30 or 60 min at different MOIs (5–20). Non-internalized bacterial cells were eliminated by three washes with PBS. In some experiments, macrophages were then incubated for 1 hr in complete medium containing 100 μg/mL gentamicin (Sigma-Aldrich) to kill extracellular bacteria and then switched to complete medium with a lower dose of gentamicin (10 μg/mL) and processed at different times post-infection. In some experiments, *S.* Typhimurium was opsonized with anti-*Salmonella* LPS IgG (Santa Cruz Biotechnology) for 2 hr at 4°C.

Determination of Macrophage Infection by Flow Cytometry

Infected cells were fixed in PBS 4% paraformaldehyde, and cells containing fluorescent bacteria (RFP+) were counted using a FacsAria I SORP sorter (Becton Dickinson). In each experiment, non-infected cells were used as internal controls of macrophage auto-fluorescence, and cells infected at 4°C were used to distinguish attached versus internalized bacteria. For more detailed information, see Supplemental Experimental Procedures.

Confocal Fluorescence Microscopy

Infected macrophages were washed with PBS and fixed with 4% paraformaldehyde for 10 min. After two additional washes with PBS, the cells were

incubated with wheat germ agglutinin (WGA)-Alexa 488 (2.5 μg/mL, 10 min) or Bodipy-fluorescein isothiocyanate (FITC) (4 μg/mL, 30 min) (Life Technologies) to stain cell membranes. In some experiments, F-actin filaments were stained with phalloidin-Alexa 633 (Life Technologies) (10 μg/mL) for 30 min at 37°C. Cell nuclei were stained with DAPI (1 μg/mL) for 5 min, whereas intracellular bacteria were detected by RFP emission. The cells were mounted in Vectashield (Vector Laboratories). Confocal images and z stack sections were acquired using Leica TCS SP2 and SP5 confocal microscopes (Leica Microsystems) and processed with ImageJ software. Five random fields per coverslip were recorded and, in each experiment, at least triplicate coverslips were generated for each condition.

In Vivo Infection

In experiments evaluating the clinical signs of infection, adult (3–5 months old) WT, LXR-deficient, or CD38-deficient female mice were pretreated with 10% sodium bicarbonate for 10 min and then infected by oral gavage with *S.* Typhimurium (10^7 CFU in 200 μL saline solution per animal). To evaluate the effects of LXR activation on morbidity, the animals were daily administered by intraperitoneal (i.p.) injection either vehicle (DMSO) or the LXR ligand T1317 (15 mg/kg animal) dissolved in physiologic saline, starting 24 hr prior to infection. Each animal was daily monitored for weight changes and other parameters associated with infection-induced morbidity, and a clinical scoring system was defined according to the development of any of the following clinical signs (one point for each sign): >15% weight loss, severe hunched position, ruffled fur, watery eyes, or slow movement. In some experiments, the mice were sacrificed at day 4 post-infection, and the infection index in the spleen was determined. In these assays, the spleens were disaggregated through a 100-μm cell strainer, and the erythrocytes were lysed using 1X Pharm Lyse lysing solution (BD Biosciences). The splenocytes were fixed in PBS 5% paraformaldehyde, and the percentage of infected cells (containing RFP+ bacteria) was analyzed by flow cytometry. An infection index was calculated for each animal by using the following formula: infection index = (percentage of RFP+ splenocytes) × (mean fluorescence intensity in the RFP+ population). Spleen samples from non-infected mice were used as negative controls.

Irradiation and Bone Marrow Transfer

Eight-week-old C57BL/6 females were sub-lethally irradiated with two sessions of 4.5 Gy separated by 4 hr. The animals were then injected with 3×10^6 bone marrow cells from either WT or CD38-deficient female donors. These procedures were carried out at the animal facility of *Parc de Recerca Biomèdica Barcelona* (PRBB). Two months after the bone marrow transfer, the mice were treated with an LXR agonist or vehicle and infected with *S.* Typhimurium as indicated above. Blood, spleen, and bone marrow specimens from non-infected mice were used to analyze the efficiency of replacement of the hematopoietic system. In these assays, surface CD38 expression was analyzed through flow cytometry. See Supplemental Experimental Procedures for more information.

RNA Extraction and Quantitative Real-Time PCR Determination

Total RNA was extracted using TRIzol Reagent (Life Technologies) as recommended by the manufacturer. More information on cDNA synthesis and quantitative real-time PCR (real-time qPCR) can be found in Supplemental Experimental Procedures. Primers used for measuring specific gene expression are described in Table S1.

Protein Extraction and Western Blot Analysis

Cells were washed in cold PBS and lysed on ice in RIPA buffer (25 mM Tris-HCl [pH 7.6], 150 mM NaCl, 1% NP-40, 1% sodium deoxycholate, and 0.1% SDS) supplemented with protease inhibitors. The samples were processed as described in Supplemental Experimental Procedures.

NAD Cycling Activity

To determine intracellular NAD^+ levels, 3×10^6 macrophages were lysed in 10% trichloroacetic acid (TCA) (Sigma-Aldrich) by sonication. Sonicated samples were centrifuged at 12,000 rpm for 2 min. The supernatants were collected, and the pellets were resuspended in 0.2 N NaOH for protein determination. TCA extraction was performed on the supernatants by adding 2 vol 1,1,2-trichloro-1,2,2-trifluroethane and 3 vol trioctylamine. After phase separation, the top aqueous layer containing NAD^+ was recovered, and its pH was adjusted to 8.0. In a 96-well plate, 100 μL of each sample diluted in water was mixed with 100 μL of a cycling reagent solution (100 mM NaH_2PO_4 [pH 8], 0.76% ethanol, 4 μM riboflavin 5′-monophosphate, 27.2 U/mL alcohol dehydrogenase, 0.24 U/mL diaphorase, and 8 μM resazurin) and incubated for 20 min in the dark. The samples were monitored every min for 60 min in a fluorescence plate reader (excitation wavelength = 544 nm; emission wavelength = 590 nm). A standard curve with known concentrations of NAD^+ was used to determine the amount of NAD^+ in the processed samples. The data were normalized by the amount of protein in each sample.

NADase Activity

NADase activity was measured using a fluorescence-based assay. In each sample, 5×10^6 macrophages were lysed by sonication in Sucrose-Tris buffer (0.25 M sucrose, 40 mM Tris [pH 7.4], and protease inhibitors). The samples were excited at 300 nm and the fluorescence was measured at 410 nm. After the baseline was recorded, 80 μM of $1,N^6$-etheno-adenine dinucleotide was added to start the reaction. The emission of fluorescence was followed at 37°C every min for 1 hr in a Gemini XPS fluorescence microplate reader (Molecular Devices). NADase activity was calculated as the slope of the linear portion of the fluorescence-time curve, corrected by the amount of protein in each sample. The final results are expressed as NADase activity (df/dt) per milligram protein. For each experimental condition, duplicate samples were processed.

Statistical Analysis

Statistical analyses were performed with SPSS software (IBM). For data with normal distribution, an ANOVA Bonferroni test or a Student's t test was used to determine statistical differences between multiple or paired comparisons, respectively. Instead, a Kruskal-Wallis Dunn's test or a Mann-Whitney *U* Wilcoxon test was used for data without normal distribution. In experiments evaluating changes of body weight along the course of infection, a repeated-measures two-way ANCOVA was used, adjusting for weight at day 0 of infection. Differences were considered significant when $p < 0.05$.

To make different experiments comparable in Figures 1A and 2C, the data were normalized using the following procedure. The intensity of each experiment (i_e) was calculated by determining the mean value of infection between the vehicle-treated control and the T1317-treated WT cells. The intensities of separate experiments were normalized by the mean intensity value of all the experiments (i_m) and, for each experiment, the resulting normalization factor (i_m/i_e) was multiplied with the percentage of infected cells of all the samples in that experiment. Similar calculations were applied to Figures 3G, 3L, 4D, and 4G.

The accession number for the microarray datasets reanalyzed in this work is MIAMExpress: E-MEXP-3871 (Pascual-García et al., 2013).

SUPPLEMENTAL INFORMATION

Supplemental Information includes Supplemental Experimental Procedures, seven figures, and one table and can be found with this article online at http://dx.doi.org/10.1016/j.celrep.2017.01.007.

AUTHOR CONTRIBUTIONS

Conceptualization, J.M., E.N.C., and A.F.V.; Methodology, J.M., F.S., S.P., L.S., S.M.-R., J. Serret, K.K., R.V., and A.F.V.; Formal Analysis, J.M., E.G., R.V., and A.F.V.; Investigation, J.M., E.G., M.B., C.E., J.M.C., K.K., R.V., T.L., M.P.-G., L.S., and A.F.V.; Validation, S.B. and A.C.; Resources, A.R., A.J., L.L., C.C., and J. Sancho; Writing–Original Draft, J.M., A.C., E.N.C., and A.F.V.; Writing–Review & Editing, C.E., M.R.S., and A.F.V.; Visualization, J.M., E.G., and A.F.V.; Supervision, E.N.C. and A.F.V.; Project Administration, A.F.V.; Funding Acquisition, C.E., R.V., C.C., and A.F.V.

ACKNOWLEDGMENTS

We thank D. Mangelsdorf for the LXR-deficient mice, J.H. Brumell for the pBR.RFP.1 plasmid, M. Sorribas and M. García for technical assistance, and A. Kupz, A. Dorhoi, and J.M. Caballero for protocols and scientific discussion. This work was supported by grants from the Spanish MICINN to A.F.V. (SAF2010-14989, SAF2011-23402, and SAF2014-57856), R.V. (SAF2010-16725), and the NuRCaMeIn network (SAF2015-71878-REDT); from Fundació la Marató de TV3 to A.F.V. (080930) and R.V. (20134030); and from COST Action BM1404 (Mye-EUNITER). M.R.S. is a Miguel Servet II researcher (ISCIII CPII14/00021), and C.E. is supported by a grant from ANII (INNOVA II, FCE_1_2014_1_104002, Uruguay). J.M. received fellowships from the Spanish MICINN (FPI, BES-2009-014828) and from the Institut Pasteur-Pierre Ledoux Jeunesse Internationale Foundation, M.P. received fellowships from the Spanish MEC (FPU, AP 2007-00821), J.M.C. received fellowships from the UB (APIF), and M.B. received fellowships from ANII (Uruguay).

Received: January 29, 2016
Revised: November 11, 2016
Accepted: January 5, 2017
Published: January 31, 2017

REFERENCES

A-Gonzalez, N., Bensinger, S.J., Hong, C., Beceiro, S., Bradley, M.N., Zelcer, N., Deniz, J., Ramirez, C., Díaz, M., Gallardo, G., et al. (2009). Apoptotic cells promote their own clearance and immune tolerance through activation of the nuclear receptor LXR. Immunity *31*, 245–258.

Aksoy, P., White, T.A., Thompson, M., and Chini, E.N. (2006). Regulation of intracellular levels of NAD: a novel role for CD38. Biochem. Biophys. Res. Commun. *345*, 1386–1392.

Alpuche-Aranda, C.M., Berthiaume, E.P., Mock, B., Swanson, J.A., and Miller, S.I. (1995). Spacious phagosome formation within mouse macrophages correlates with Salmonella serotype pathogenicity and host susceptibility. Infect. Immun. *63*, 4456–4462.

Belenky, P., Bogan, K.L., and Brenner, C. (2007). NAD+ metabolism in health and disease. Trends Biochem. Sci. *32*, 12–19.

Castrillo, A., Joseph, S.B., Vaidya, S.A., Haberland, M., Fogelman, A.M., Cheng, G., and Tontonoz, P. (2003). Crosstalk between LXR and toll-like receptor signaling mediates bacterial and viral antagonism of cholesterol metabolism. Mol. Cell *12*, 805–816.

Chini, E.N. (2009). CD38 as a regulator of cellular NAD: a novel potential pharmacological target for metabolic conditions. Curr. Pharm. Des. *15*, 57–63.

Drach, J., McQueen, T., Engel, H., Andreeff, M., Robertson, K.A., Collins, S.J., Malavasi, F., and Mehta, K. (1994). Retinoic acid-induced expression of CD38 antigen in myeloid cells is mediated through retinoic acid receptor-alpha. Cancer Res. *54*, 1746–1752.

Ghisletti, S., Huang, W., Ogawa, S., Pascual, G., Lin, M.-E., Willson, T.M., Rosenfeld, M.G., and Glass, C.K. (2007). Parallel SUMOylation-dependent pathways mediate gene- and signal-specific transrepression by LXRs and PPARgamma. Mol. Cell *25*, 57–70.

Gold, E.S., Diercks, A.H., Podolsky, I., Podyminogin, R.L., Askovich, P.S., Treuting, P.M., and Aderem, A. (2014). 25-Hydroxycholesterol acts as an amplifier of inflammatory signaling. Proc. Natl. Acad. Sci. USA *111*, 10666–10671.

Guiney, D.G., and Lesnick, M. (2005). Targeting of the actin cytoskeleton during infection by Salmonella strains. Clin. Immunol. *114*, 248–255.

Haas, A. (2007). The phagosome: compartment with a license to kill. Traffic *8*, 311–330.

Haraga, A., Ohlson, M.B., and Miller, S.I. (2008). Salmonellae interplay with host cells. Nat. Rev. Microbiol. *6*, 53–66.

Hardt, W.D., Chen, L.M., Schuebel, K.E., Bustelo, X.R., and Galán, J.E. (1998). S. typhimurium encodes an activator of Rho GTPases that induces membrane ruffling and nuclear responses in host cells. Cell *93*, 815–826.

Hong, C., and Tontonoz, P. (2014). Liver X receptors in lipid metabolism: opportunities for drug discovery. Nat. Rev. Drug Discov. *13*, 433–444.

Iqbal, J., and Zaidi, M. (2006). TNF regulates cellular NAD+ metabolism in primary macrophages. Biochem. Biophys. Res. Commun. *342*, 1312–1318.

Ito, A., Hong, C., Rong, X., Zhu, X., Tarling, E.J., Hedde, P.N., Gratton, E., Parks, J., and Tontonoz, P. (2015). LXRs link metabolism to inflammation through Abca1-dependent regulation of membrane composition and TLR signaling. eLife *4*, e08009.

Janowski, B.A., Grogan, M.J., Jones, S.A., Wisely, G.B., Kliewer, S.A., Corey, E.J., and Mangelsdorf, D.J. (1999). Structural requirements of ligands for the oxysterol liver X receptors LXRalpha and LXRbeta. Proc. Natl. Acad. Sci. USA *96*, 266–271.

Joseph, S.B., Bradley, M.N., Castrillo, A., Bruhn, K.W., Mak, P.A., Pei, L., Hogenesch, J., O'connell, R.M., Cheng, G., Saez, E., et al. (2004). LXR-dependent gene expression is important for macrophage survival and the innate immune response. Cell *119*, 299–309.

Kiama, S.G., Dreher, D., Cochand, L., Kok, M., Obregon, C., Nicod, L., and Gehr, P. (2006). Host cell responses of Salmonella typhimurium infected human dendritic cells. Immunol. Cell Biol. *84*, 475–481.

Korf, H., Vander Beken, S., Romano, M., Steffensen, K.R., Stijlemans, B., Gustafsson, J.-Å., Grooten, J., and Huygen, K. (2009). Liver X receptors contribute to the protective immune response against Mycobacterium tuberculosis in mice. J. Clin. Invest. *119*, 1626–1637.

Lala, D.S., Syka, P.M., Lazarchik, S.B., Mangelsdorf, D.J., Parker, K.L., and Heyman, R.A. (1997). Activation of the orphan nuclear receptor steroidogenic factor 1 by oxysterols. Proc. Natl. Acad. Sci. USA *94*, 4895–4900.

Lee, J.H., Park, S.M., Kim, O.S., Lee, C.S., Woo, J.H., Park, S.J., Joe, E.H., and Jou, I. (2009). Differential SUMOylation of LXRalpha and LXRbeta mediates transrepression of STAT1 inflammatory signaling in IFN-gamma-stimulated brain astrocytes. Mol. Cell *35*, 806–817.

Lee, C.-U., Song, E.-K., Yoo, C.-H., Kwak, Y.-K., and Han, M.-K. (2012). Lipopolysaccharide induces CD38 expression and solubilization in J774 macrophage cells. Mol. Cells *34*, 573–576.

Lilic, M., Galkin, V.E., Orlova, A., VanLoock, M.S., Egelman, E.H., and Stebbins, C.E. (2003). Salmonella SipA polymerizes actin by stapling filaments with nonglobular protein arms. Science *301*, 1918–1921.

Lischke, T., Heesch, K., Schumacher, V., Schneider, M., Haag, F., Koch-Nolte, F., and Mittrücker, H.-W. (2013). CD38 controls the innate immune response against Listeria monocytogenes. Infect. Immun. *81*, 4091–4099.

Luo, L., Wall, A.A., Yeo, J.C., Condon, N.D., Norwood, S.J., Schoenwaelder, S., Chen, K.W., Jackson, S., Jenkins, B.J., Hartland, E.L., et al. (2014). Rab8a interacts directly with PI3Kγ to modulate TLR4-driven PI3K and mTOR signalling. Nat. Commun. *5*, 4407.

McWhorter, F.Y., Wang, T., Nguyen, P., Chung, T., and Liu, W.F. (2013). Modulation of macrophage phenotype by cell shape. Proc. Natl. Acad. Sci. USA *110*, 17253–17258.

Musso, T., Deaglio, S., Franco, L., Calosso, L., Badolato, R., Garbarino, G., Dianzani, U., and Malavasi, F. (2001). CD38 expression and functional activities are up-regulated by IFN-gamma on human monocytes and monocytic cell lines. J. Leukoc. Biol. *69*, 605–612.

Partida-Sánchez, S., Cockayne, D.A., Monard, S., Jacobson, E.L., Oppenheimer, N., Garvy, B., Kusser, K., Goodrich, S., Howard, M., Harmsen, A., et al. (2001). Cyclic ADP-ribose production by CD38 regulates intracellular calcium release, extracellular calcium influx and chemotaxis in neutrophils and is required for bacterial clearance in vivo. Nat. Med. *7*, 1209–1216.

Pascual-García, M., Rué, L., León, T., Julve, J., Carbó, J.M., Matalonga, J., Auer, H., Celada, A., Escolà-Gil, J.C., Steffensen, K.R., et al. (2013). Reciprocal negative cross-talk between liver X receptors (LXRs) and STAT1: effects on IFN-γ-induced inflammatory responses and LXR-dependent gene expression. J. Immunol. *190*, 6520–6532.

Price, J.V., and Vance, R.E. (2014). The macrophage paradox. Immunity *41*, 685–693.

Reboldi, A., Dang, E.V., McDonald, J.G., Liang, G., Russell, D.W., and Cyster, J.G. (2014). Inflammation. 25-Hydroxycholesterol suppresses interleukin-1-driven inflammation downstream of type I interferon. Science *345*, 679–684.

Sanjurjo, L., Amézaga, N., Aran, G., Naranjo-Gómez, M., Arias, L., Armengol, C., Borràs, F.E., and Sarrias, M.-R. (2015). The human CD5L/AIM-CD36 axis: a novel autophagy inducer in macrophages that modulates inflammatory responses. Autophagy *11*, 487–502.

Song, E.-K., Lee, Y.-R., Kim, Y.-R., Yeom, J.-H., Yoo, C.-H., Kim, H.-K., Park, H.-M., Kang, H.-S., Kim, J.-S., Kim, U.-H., and Han, M.K. (2012). NAADP mediates insulin-stimulated glucose uptake and insulin sensitization by PPARγ in adipocytes. Cell Rep. *2*, 1607–1619.

Spann, N.J., Garmire, L.X., McDonald, J.G., Myers, D.S., Milne, S.B., Shibata, N., Reichart, D., Fox, J.N., Shaked, I., Heudobler, D., et al. (2012). Regulated accumulation of desmosterol integrates macrophage lipid metabolism and inflammatory responses. Cell *151*, 138–152.

Sun, K., and Metzger, D.W. (2008). Inhibition of pulmonary antibacterial defense by interferon-gamma during recovery from influenza infection. Nat. Med. *14*, 558–564.

Valledor, A.F., Hsu, L.-C., Ogawa, S., Sawka-Verhelle, D., Karin, M., and Glass, C.K. (2004). Activation of liver X receptors and retinoid X receptors prevents bacterial-induced macrophage apoptosis. Proc. Natl. Acad. Sci. USA *101*, 17813–17818.

Venter, G., Oerlemans, F.T.J.J., Willemse, M., Wijers, M., Fransen, J.A.M., and Wieringa, B. (2014). NAMPT-mediated salvage synthesis of NAD+ controls morphofunctional changes of macrophages. PLoS ONE *9*, e97378.

Viegas, M.S., do Carmo, A., Silva, T., Seco, F., Serra, V., Lacerda, M., and Martins, T.C. (2007). CD38 plays a role in effective containment of mycobacteria within granulomata and polarization of Th1 immune responses against Mycobacterium avium. Microbes Infect. *9*, 847–854.

Wagner, B.L., Valledor, A.F., Shao, G., Daige, C.L., Bischoff, E.D., Petrowski, M., Jepsen, K., Baek, S.H., Heyman, R.A., Rosenfeld, M.G., et al. (2003). Promoter-specific roles for liver X receptor/corepressor complexes in the regulation of ABCA1 and SREBP1 gene expression. Mol. Cell. Biol. *23*, 5780–5789.

Wang, Z., Zhou, S., Sun, C., Lei, T., Peng, J., Li, W., Ding, P., Lu, J., and Zhao, Y. (2014). Interferon-γ inhibits nonopsonized phagocytosis of macrophages via an mTORC1-c/EBPβ pathway. J. Innate Immun. *7*, 165–176.

Yin, H., van der Veer, E., Frontini, M.J., Thibert, V., O'Neil, C., Watson, A., Szasz, P., Chu, M.W.A., and Pickering, J.G. (2012). Intrinsic directionality of migrating vascular smooth muscle cells is regulated by NAD(+) biosynthesis. J. Cell Sci. *125*, 5770–5780.